GEOPHYSICAL RESEARCH LETTERS, VOL. 26, NO. 21, PAGES 3293-3296, NOVEMBER 1, 1999

Modeling the relaxation of red sprite plasma

David Nunn

Department of Electronics and Computer Science, University of Southampton, United Kingdom.

Craig J. Rodger

British Antarctic Survey, Cambridge, United Kingdom.

Abstract. Red sprites consist of multiple ionised columns extending above a thunderstorm from ~30 km to ~90 km. Electron densities in these columns are very much larger than the ambient background, perhaps fives orders of magnitude at 70 km. These highly ionized structures cause observable perturbations in subionospheric VLF transmissions known as "VLF Sprites". Three models of initial sprite electron density are considered, and using a realistic ionization relaxation model the time dependence of electron density is derived. A 3-D Born propagation code of is used to compute the time profile of a VLF sprite. Two profiles show good agreement with the time signature experimentally observed, in that scattered amplitude and phase decrease logarithmically with time. These simulations provide insight into the nature and structure of sprite columns, and indicate an additional constraint which should be applied to red sprite creation models.

1. Introduction

Red sprites are observed as clusters of short-lived (~50 ms) pinkish-red luminous columns, stretching from ~30 km to ~85 km altitude, and < 1 km wide. Red sprite observations have been made from the ground, from aircraft, and the U. S. Space Shuttle [see *Rodger*, 1999]. There is now strong evidence that red sprites are closely associated with plasma columns with large electron densities in comparison with the ambient night-time ionosphere. The first evidence for this came from observations of VLF Sprites [*Dowden et al.*, 1996a, b] and subsequent modeling suggesting that the difference in electron densities could be nearly five orders of magnitude larger than ambient at ~70 km altitude [*Rodger and Nunn*, 1999]. This finding is supported by recent spectral measurements of red sprites reported at the 1998 AGU Fall meeting [e.g., *Heavner et al.*, 1998]. There is some controversy in this area and these findings are not accepted by all researchers [e. g., *Inan et al.*, 1996].

"VLF sprites" are perturbations observed in the phase and amplitude of subionospheric VLF transmissions associated spatially and temporally with red sprites [*Dowden et al.*, 1996a], and are observed simultaneously on widely separated transmission paths and require high angle scattering. Another defining characteristic is the temporal signature of the perturbation. Recent observations of VLF sprites showed that the amplitude of the perturbation phasor (the "echo" amplitude) decayed logarithmically with time [*Dowden et al.*, 1997]. During the decay the phase of the perturbation phasor (the "echo" phase) varied monotonically and also logarithmically with time. The time after which the perturbation decayed into the background noise was typically 30 - 100 s. This temporal signature has been explained through the scattering caused by an ionized column in the Earth-ionosphere waveguide that becomes progressively shorter as the ionization relaxes back to ambient conditions [*Dowden and Rodger*, 1997].

In this paper we examine the relaxation of a column of plasma placed inside the Earth-ionosphere waveguide and apply a fully 3-D propagation model [*Nunn*, 1997] to calculate the temporal signature of the resulting VLF perturbation.

2. Relaxation of Red Sprite Plasma

In our formulation we take an extremely simple model of a red sprite; a single column of ionization (or "spritelet") inside the Earth-ionosphere waveguide. The effects of multiple columns of ionization in the production of VLF sprites has been most recently considered by *Rodger and Nunn* [1999], but in order to investigate the temporal signature produced by the scattering of VLF transmission from relaxing red sprite plasma we need only consider a single column. The additional free electron density in the red sprite plasma $dN_e(x, y, z)$ is superimposed upon the ambient night-time distribution $N_e(z)$, in our case a Wait ionosphere [*Wait and Spies*, 1964] specified by $h' = 84$ km and $\beta = 0.5$ km^{-1}. The horizontal dependence of dN_e is taken to be an 8th order Butterworth function with a spritelet radius $a = 300$ m (following *Rodger and Nunn* [1999]) which produces a nearly "straight-edged" column. The profile for the effective electron-neutral collision frequency $\upsilon_{eff}(z)$ is that of *Morfitt and Shellman* [1976]. For these calculations we follow *Rodger and Nunn* [1999] and assume that there is no perturbation in $\upsilon_{eff}(z)$ within the spritelet.

The electron densities profiles (dN_e + N_e) used in our calculations are shown in Figure 1. The figure shows the maximum electron densities at the centre of the spritelet at $t = 0$, before the ionization starts to relax. Profile A is taken from Figure 4 of *Rodger and Nunn* [1999]. The earlier modeling of *Dowden and Rodger* [1997] relied upon a propagation model with one spatial dimension plus time, requiring that the sprite plasma have constant conductivity at all altitudes, a substantial limitation not present in this 3D approach. Profile B was that used by *Dowden and Rodger* [1997] to produce an altitude independent conductivity, and is included to provide comparison with earlier work in this area.

Copyright 1999 by the American Geophysical Union.

Paper number 1999GL003578.
0094-8276/99/1999GL003578$05.00

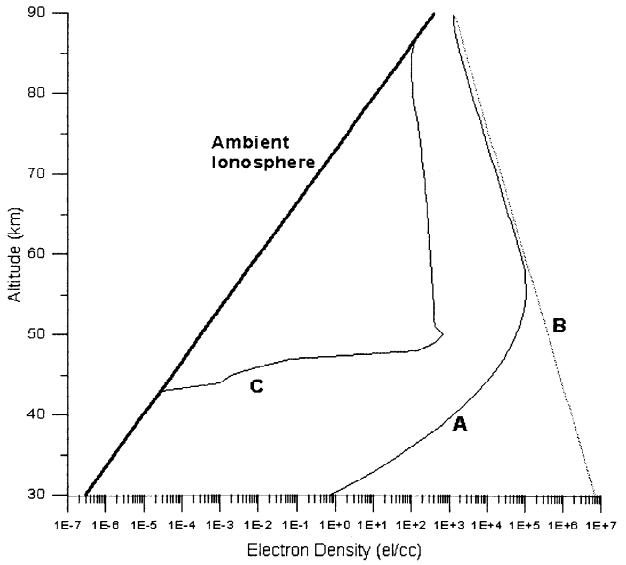

Figure 1. The height dependence of the electron density (per cubic centimetre) profiles used in this study, as described in the text. The figure shows the ambient night-time electron density N_e and the total electron densities ($dN_e + N_e$) at the centre of the spritlet at $t = 0$.

The very large densities at low altitudes are clearly not physical in this situation, but would in any case be removed within 1 ms (the minimum time used in our calculations). Profile C is derived from Figure 2a ($t = 20$ ms) of *Pasko et al.* [1996]. The relaxation of dN_e back to ambient levels is calculated using the expressions found in *Rodger et al.* [1998], along with the ambient parameters from CIRA-1986 [*Labitzke et al.*, 1990] for July at latitude 40°N. The calculations here assume that the positive ions associated with the red sprite will not become hydrated cluster ions before they undergo dissociative recombination. The ionization relaxation model of *Rodger et al.* [1998] was also used by *Dowden and Rodger* [1997b] in a simplified form. Figure 2 shows the relaxing electron density profile A at times $t = 0$, 0.01, 0.1, 1, 10 and 100 s. Significant ionization is present above 75 km even after 100 s for this sprite profile.

3. The Numerical Modeling

Calculations are made for the path from the VLF transmitter NLK (Seattle, 48°12'15" N, 121°55'00" W, 24.8 kHz) to Yucca Ridge, Colorado (1600 km path length), where annual red sprite research campaigns have been conducted and red sprite-associated VLF perturbations have been observed. The model for the ground used is that for the Great Plains of the USA ($\sigma = 10$ mSm^{-1} and $\varepsilon_r = 15$) [*Morgan*, 1968]. The spritelet is positioned on the Great Circle Path (GCP) 500 km from Yucca Ridge in the direction of NLK. For the purposes of this study we will restrict ourselves to a single column position at this distance on the GCP (thus with zero scattering angle), although there is nothing unique about this position.

The propagation calculations use the numerical model of *Nunn* [1997]. This is a 3D realistic propagation model using Wait's modal propagation theory [*Wait*, 1970], with a curved Earth and a realistic ionosphere and ground. Propagation is handled in the code using the NOSC MODEFNDR code [*Morfitt and Shellman*, 1976]. For this problem MODEFNDR returned 22 TM and TE modes in all, and the code uses all of these and computes a full inter-modal scattering matrix at the scatterer. Modal propagation theory is certainly valid at the range of 500 km if enough modes are included in the calculations, confirmed by examining the modal composition of the scattered field at the receiver where the amplitude of the highest order modes were found to be negligible. The theoretical basis of the Nunn code is a 3D Born weak scattering formalism. It is necessary to take account of the fact that a sprite column is a strong non-Born scatterer. The formulation is however rigorous in the limit that the assumed zero-order incident field in the code is the field existing at that point in the presence of the scatterer. *Rodger et al.* [1998] undertook theoretical analysis for the case of a "thin" infinitely long conducting cylinder orientated at right angles to an incident plane EM wave giving analytic expressions for the prevailing field at the cylinder surface as a complex fraction of the "zero-order" incident field, providing the so-called self-shielding factor. This factor takes into account the fact that the field at the surface of the cylinder may be substantially modified by the vertical currents induced in the column. Furthermore, *Rodger et al.* [1998] gave analytically the dependence of electric field on radius within the column (skin depth effect). The incident zero-order field in the 3D Born code is modified by the self-shielding term and uses a realistic the radial dependence within the column.

4. Results.

For the modeling parameters detailed above, and using profile A, Figure 3a plots scattered field amplitude measured as a fraction of the direct propagation field as a function of $\log_{10}(t)$. The calculations cover the time range 1 ms-100 s. For

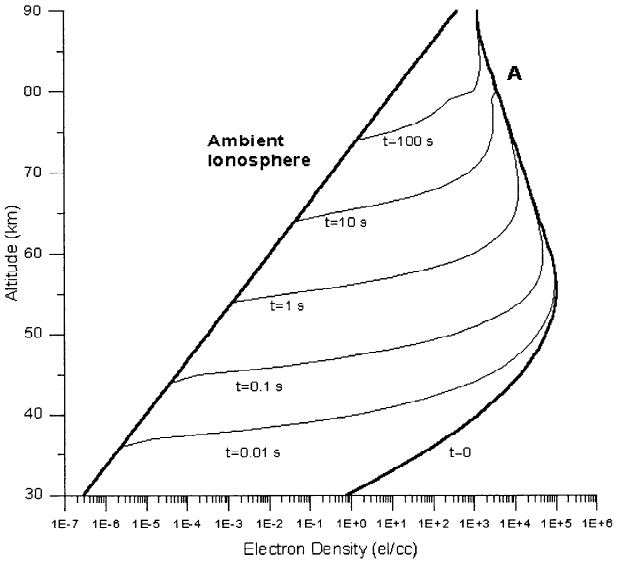

Figure 2. Relaxation of the red sprite electron density profile A (Figure 1) with time. Once again the central electron density is presented.

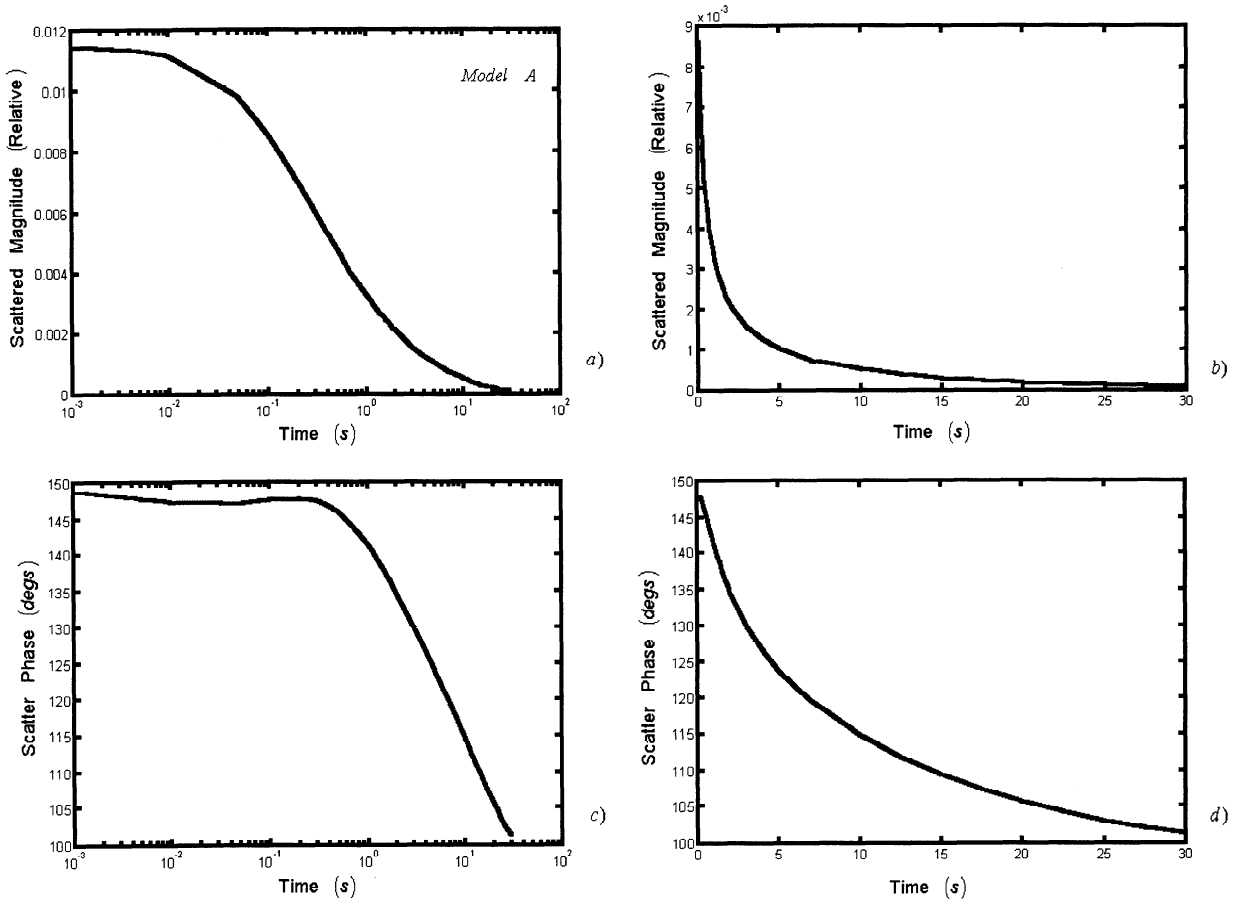

Figure 3. Relative amplitude (a) and phase (d) of the scattered field as a function of log(t), for the case of forward scattering from 1 column at a range of 500 km. The profile model used is that of *Nunn and Rodger* (A). The dependence of these quantities as a function of t is shown in b) and d). The functional dependence on time is as observed in the experimental data. The functional dependence on time is as observed in the experimental data.

timescales < 1 ms the plasma will be very hot and computations would require consideration of the perturbation of collision frequency. However the time resolution of the experimental equipment used to study VLF sprites is ~0.1 s and so changes on a smaller timescale than this will be currently unobservable. This quantity, the "scattered amplitude (relative)", decreases monotonically with time as expected, and effectively terminates the observable VLF sprite after about 50 s. In the time range 0.1 - 5 s the dependence on log(t) is linear, in good agreement with the results of *Dowden et al.*[1997]. This is explained by the upward collapse of the electron density column into the ionosphere due to relaxation, as predicted by the slab model of *Dowden and Rodger* [1997]. At larger times scattered amplitude acquires a decaying exponential dependence on log(t). This departure from pure log(t) dependence is due to destructive interference of signals scattered from different parts of column. This transition is likely to occur near the noise limit of experimental observations and is not seen in the experimental data of *Dowden et al.* [1997]. Figure 3b plots the same quantity as a function of linear time, and again shows the same characteristics found in earlier experimental reports.

Figure 3c plots scatter phase as a function of log(t). Beyond t = 0.5 s the phase shows an almost exactly linear decrease with log(t), the total decrease over the duration of the event being ~ 50 degs. This result is in extremely good agreement with those in *Dowden et al.* [1997], and is readily understood. It was shown in *Nunn* [1997] that the scatter phase of a low altitude resistive body on the GLC path is 225°. However, in the case of scattering from the upper part of the column the ray paths have longer path lengths through the ionospheric plasma and will have an average extra lag of ~ 75°, which gives the initial scatter phase of 150 degrees. As the column collapses upwards with time scattering from high altitudes will predominate and overall scattered field phase will steadily decrease. Figure 3d shows scattered field phase as a function of linear time, which is in good agreement with observations in *Dowden et al.* [1997]. It was also pointed out by *Dowden* [1996] that high altitude winds ~100 ms^{-1} can give a significant additional linear dependence of scattered phase on time, or doppler shift, but this effect has not been considered in this paper.

It can be seen from Figure 3a that the initial scattered field strength is ~ -39 dB. With scattered phase in the quadrant 90-180° this will produce a negative amplitude, positive phase VLF sprite of ~ -0.1 dB and 0.4°. In separate numerical calculations the sprite was modeled as a collection of 15 columns, scattered over an area ~ 20 km^2 (see *Rodger and Nunn* [1999] for the distributions used in this modeling and more discussion into multiple columns). When the column assembly is located on the GLC path, the path differences for scattering from different columns are small, and the overall computed VLF sprites are very similar in form to those of the

one column case, except that amplitudes are multiplied by a factor ~ 15. The resultant VLF sprites then have maximum amplitude perturbations of order -0.3 dB, and phase perturbations of order 6 degrees, figures in good general agreement with observed values. Numerical modeling using profile B gave results very similar to profile A (not shown), the main difference being that the scatter phase as a function of log(t) is more advanced (positive) at small times <0.1 s. Calculations using profile C (not shown) produced a time dependency of scattered field amplitude which showed some agreement with *Dowden et al.* [1998], although this was poor in comparison with profiles A and B. The overall scattered field strength for profile C was far too low to give a measurable VLF sprite, at least for a column radius of 300 m. The dependence of scatter phase on log(t) was found to depart considerably from linear, and in fact scatter phase decreased almost exactly linearly with t. Such a decay signature has not been reported in the literature, and is quite different from the logarithmic decay of VLF sprites described by *Dowden et al* [1997]. This modeling suggests a new method to test red sprite creation mechanisms. A red sprite mechanism should not be limited to producing an event with the appropriate optical properties. The electrical properties must be able to produce VLF perturbations with complex structure and significant amplitude, and also create an electron density profile that will produce a VLF sprite with log decay. It is not clear that the calculations which produced profile C meet all these requirements.

5. Conclusion

In this paper we have modeled numerically the time signature of a VLF sprite, for a single 3D sprite column on the GLC path. Using three models for initial sprite electron density as a function of height, and a suitable model for the recombination rate as a function of height, VLF sprite time signatures were obtained. Two of these showed the functional form observed in the field by Dowden and co-workers, namely a linear dependence on log(t) of scattered amplitude and a linear decrease of scattered phase with log(t). For these profiles the overall predicted amplitudes of VLF sprites are in good agreement with observations. This suggests that these electron density profiles are of the right form and order. It is not clear that the third profile, taken from *Pasko et al.* [1996], can produce VLF sprites with the observed properties. These simulations provide insight into the nature and structure of sprite columns, as well as an additional test which should be considered when evaluating the validity of various red sprite creation models. For example, recent theoretical work has provided important insight into the fine-scale structure of red sprites through streamer mechanisms [*Pasko et al.*, 1998]. However, it is difficult to test the results of this work until it has been combined with overall red sprite and electron density profiles calculated.

Acknowledgments. One of the authors (CJR) was supported by New Zealand Science and Technology Postdoctoral Fellowship Contract BAS 701. One author (DN) thanks Churchill College Cambridge for their support for this project. The authors would like to thank Richard L. Dowden of the University of Otago for helpful discussions.

References

Dowden, R. L., Distortion of Trimpi shapes by high altitude winds, *J. Geophys. Res., 101*, 315-321, 1996.

Dowden, R. L., and C. J. Rodger, Decay of a vertical plasma column: A model to explain VLF sprites, *Geophys. Res. Lett., 24*, 2765-2768, 1997.

Dowden, R. L., J. B. Brundell, W. A. Lyons, and T. Nelson, Detection and location of red sprites by VLF scattering of subionospheric transmissions, *Geophys. Res. Lett., 23*, 1737-1740, 1996a.

Dowden, R. L., J. B. Brundell, and C. J. Rodger, Temporal evolution of very strong Trimpis observed at Darwin, Australia, *Geophys. Res. Lett., 24*, 2419-2422, 1997

Heavner, M. J., D. D. Sentman, E. M. Westcott, J. S. Morrill, C. Siefring, E. J. Bucsela, D. L. Osborne, J. T. Desrochers, H. Nielson, J. Winick, J. Kristl, T. Hudson, L. M. Peticolas and V. Besser, Ionisation in Sprites, *Eos, Trans.*, F165, 1998.

Inan, U. S., T. F. Bell, and V. P. Pasko, Reply, *Geophys. Res. Lett., 23*, 3421-3422, 1996.

Labitzke, K., J. J. Barnett, and D. Rees (editors), CIRA 1986; COSPAR International Reference Atmosphere 1986, *Adv. Space Res., 10*, 12, 1990.

Morfitt, D. G., and C. H. Shellman, MODESRCH, an improved computer program for obtaining ELF/VLF/LF propagation data, *Naval Ocean Systems Center Tech. Report. NOSC/TR 141*, NTIS Accession No. ADA047508, National Technical Information Service, Springfield, VA 22161, U.S.A, 1976.

Morgan, R. R., World-wide VLF effective-conductivity map, *Westinghouse Report 80133F-1*, submitted to the Office of Naval Research, Washington D.C. 20360, 1968.

Nunn, D., On the numerical modelling of the VLF Trimpi effect, *J. Atmos. Terr. Phys., 59*(5), 537-560, 1997.

Pasko, V. P., U. S. Inan, T. F. Bell, Spatial structure of sprites, *Geophys. Res. Lett., 25*, 2123-2126, 1998.

Pasko, V. P., U. S. Inan, and T. F. Bell, Sprites as luminous columns of ionisation produced by quasi-electrostatic thundercloud fields, *Geophys. Res. Lett., 23*, 649-652, 1996.

Rodger, C. J., Red sprites, upward lightning and VLF perturbations, *Rev. Geophys.*, 37,317-336, 1999.

Rodger, C. J., J. R. Wait, and R. L. Dowden, VLF scattering from red sprites-Theory, *J. Atmos. Solar-Terr. Phys., 60*, 755-763, 1998.

Rodger, C. J., and D. Nunn, VLF scattering from red sprites: Application of numerical modeling, *Radio Sci.*, 34, 923-932, 1999.

Rodger, C. J., O. A. Molchanov, and N. R. Thomson, Relaxation of transient ionization in the lower ionosphere, *J. Geophys. Res., 103*, 6969-6975, 1998.

Wait, J. R., *Electromagnetic Waves in Stratified Media*, Pergamon Press, New York, 1970.

Wait, J.R. and K.P. Spies, Characteristics of the Earth-ionosphere waveguide for VLF radio waves, Tech. Note 300, National Bureau of Standards, 1964.

D. Nunn, Department of Electronics and Computer Science, University of Southampton, Highfield, Southampton SO17 1BJ, United Kingdom. (e-mail: D.Nunn@ecs.soton.ac.uk)

C. J. Rodger, Physical Sciences Division, British Antarctic Survey, High Cross, Madingley Road, Cambridge CB3 0ET, United Kingdom. (e-mail: cjro@mail.nerc-bas.ac.uk)

(Received April 28, 1999; revised September 20, 1999; accepted September 23, 1999.)